Intratumor T helper type 2 cell infiltrate correlates with cancer-associated fibroblast thymic stromal lymphopoietin production and reduced survival in pancreatic cancer

Lucia De Monte,[1,6] Michele Reni,[2,7] Elena Tassi,[1,6] Daniela Clavenna,[3,7] Ilenia Papa,[3,7] Helios Recalde,[4] Marco Braga,[5,7,8] Valerio Di Carlo,[5,7,8] Claudio Doglioni,[3,7,8] and Maria Pia Protti[1,6]

[1]Tumor Immunology Unit, [2]Clinical Oncology Unit, [3]Pathology Unit, [4]Blood Bank, [5]Pancreas Unit, [6]Division of Immunology, Transplantation and Infectious Diseases, and [7]Division of Molecular Oncology, San Raffaele Scientific Institute, 20132 Milan, Italy
[8]San Raffaele Vita-Salute University, 20132 Milan, Italy

Pancreatic cancer is a very aggressive disease characterized by a marked desmoplasia with a predominant Th2 (GATA-3+) over Th1 (T-bet+) lymphoid infiltrate. We found that the ratio of GATA-3+/T-bet+ tumor–infiltrating lymphoid cells is an independent predictive marker of patient survival. Patients surgically treated for stage IB/III disease with a ratio inferior to the median value had a statistically significant prolonged overall survival, implying an active role for Th2 responses in disease progression. Thymic stromal lymphopoietin (TSLP), which favors Th2 cell polarization through myeloid dendritic cell (DC) conditioning, was secreted by cancer-associated fibroblasts (CAFs) after activation with tumor–derived tumor necrosis factor α and interleukin 1β. TSLP-containing supernatants from activated CAFs induced in vitro myeloid DCs to up–regulate the TSLP receptor (TSLPR), secrete Th2-attracting chemokines, and acquire TSLP-dependent Th2-polarizing capability in vitro. In vivo, Th2 chemoattractants were expressed in the tumor and in the stroma, and TSLPR-expressing DCs were present in the tumor stroma and in tumor-draining but not in nondraining lymph nodes. Collectively, this study identifies in pancreatic cancer a cross talk between tumor cells and CAFs, resulting in a TSLP-dependent induction of Th2-type inflammation which associates with reduced patient survival. Thus, blocking TSLP production by CAFs might help to improve prognosis in pancreatic cancer.

CORRESPONDENCE
Maria Pia Protti:
m.protti@hsr.it

Abbreviations used: CAF, cancer-associated fibroblast; CI, confidence interval; G/T, GATA-3+/T-bet+; HDF, human dermal fibroblast; LCM, laser capture microdissection; MDC/CCL22, macrophage-derived chemokine; SMA, smooth muscle actin; TARC/CCL17, thymus and activation-regulated chemokine; TSLP, thymic stromal lymphopoietin; TSLPR, TSLP receptor.

Pancreatic cancer is a very aggressive disease with dismal prognosis (Hidalgo, 2010). Desmoplasia/fibrosis, which is not present around normal pancreatic ducts, is a hallmark in pancreatic cancer and it is believed to play an active role in disease progression and aggressiveness (Kleeff et al., 2007; Mahadevan and Von Hoff, 2007). Tumor stroma is predominantly infiltrated by Th2 (GATA-3+) over Th1 (T-bet+) cells (Tassi et al., 2008). This immune infiltrate correlates with the presence in the blood of pancreatic cancer patients of tumor-specific CD4+ T cells producing mostly IL-5 and IL-13 (Tassi et al., 2008). Th2 cytokines and IL-13 in particular are strongly linked to fibrogenesis (Wynn, 2004).

Open questions are what leads to the Th2 immune deviation in pancreatic cancer and whether

Th2 cells present at the tumor site have a role in disease progression. We hypothesized that tumor-resident DCs are conditioned by factors released by tumor cells or tumor stroma to favor, in the draining LNs, differentiation of tumor-specific Th2 cells, which then home to the tumor and possibly contribute to disease progression by interacting with other immune and nonimmune cells (Joyce and Pollard, 2009) and, through Th2 cytokines secretion, to fibrosis (Wynn, 2004).

The thymic stromal lymphopoietin (TSLP; i.e., an IL-7–like cytokine) has been recently

associated with induction of Th2 responses through DC activation (Liu et al., 2007). Hence, in this paper we evaluated, first, the prognostic significance of Th2-infiltrating lymphoid cells in surgical specimens of patients who had resection of stage IB/III pancreatic cancer and, second, the potential implication of TSLP in inducing the Th2 immune deviation present in pancreatic cancer.

RESULTS

The ratio of GATA-3+/T-bet+ (G/T) tumor–infiltrating lymphoid cells predicts survival after surgery in patients with stage IB/III pancreatic cancer

To determine the possible association between Th2 cells and disease progression, we enumerated by immunohistochemistry the GATA-3+ and T-bet+ lymphoid cell–infiltrating tumor samples from 69 patients who underwent surgical resection (Fig. 1 A, left). GATA-3 was also expressed in the cytoplasm of epithelial cells as already shown in Tassi et al. (2008; Fig. 1 A, top). Lymphoid cell infiltrate was mostly present exclusively in the tumor stroma and varied among samples. Pancreatic tissue from surgical samples of patients who underwent surgery for benign lesions is also shown as normal control. Compared with the tumor, in which the stromal component is very represented, normal pancreatic tissue is composed by a compact acinar structure that contains rare and equal numbers of lymphoid cells positive for GATA-3 and T-bet (Fig. 1 A, right). Because the amount of lymphoid cells in the tumor varied among samples, we then calculated for each patient the percentage of positive lymphoid cells and found that in all but one sample the percentage of GATA-3+ cells was significantly higher than that of T-bet+ (Fig. 1 B), demonstrating that Th2 immune deviation in pancreatic cancer is a generalized phenomenon. However, the percentage of intratumor

Th2 cells varied among the samples (Fig. 1 B). To verify possible quantitative differences among samples, we then calculated the G/T ratio for each patient (Fig. 1 C). Indeed, Cox regression model showed no significant correlation between overall survival and the absolute number of either GATA-3+ (hazard ratio = 1.00; 95% confidence interval [CI] 1.00–1.00; P = 0.73) or T-bet+ (hazard ratio = 1.00; 95% CI 1.00–1.00; P = 0.52) cells. Conversely, a significant correlation between G/T ratio and overall survival was detected (hazard ratio = 1.04; 95% CI 1.01–1.04; P = 0.038). The median value of G/T ratio was 5.2; 35 patients had a G/T ratio ≤ 5.2 (group A) and 34 patients had a G/T ratio > 5.2 (group B; patient characteristics grouped by the G/T ratio are reported in Table I). After a median followup of 41 mo (range 22–134), 58 patients had recurrence and 53 died from the disease. Median 1-yr and 2-yr disease-free survival was 15.2 mo, 71 and 43% for group A, and 11.0 mo, 47 and 18% for group B (P = 0.02). Median 2-yr and 3-yr overall survival was 32.7 mo, 66 and 45% for group A, and 20.2 mo, 44 and 26% in group B (P = 0.008; Fig. 1 D and Fig. S1). Multivariate analysis stratifying for tumor stage, grading, size, site, patient performance status, gender, age, surgical resection margins, postoperative CA19.9 value, and postoperative treatment confirmed that the G/T ratio was independently predictive of both disease-free survival (P = 0.002, hazard ratio = 1.06, 95% CI 1.03–1.10) and overall survival (P = 0.005, hazard ratio = 1.06, 95% CI 1.02–1.09). Hence, the GATA-3+ cells present in the tumor stroma associate with disease progression, and we identified a parameter (i.e., the G/T ratio) that is independently predictive of patients' survival.

TSLP is produced by cancer–associated fibroblasts (CAFs) after activation by tumor–derived TNF and IL-1β

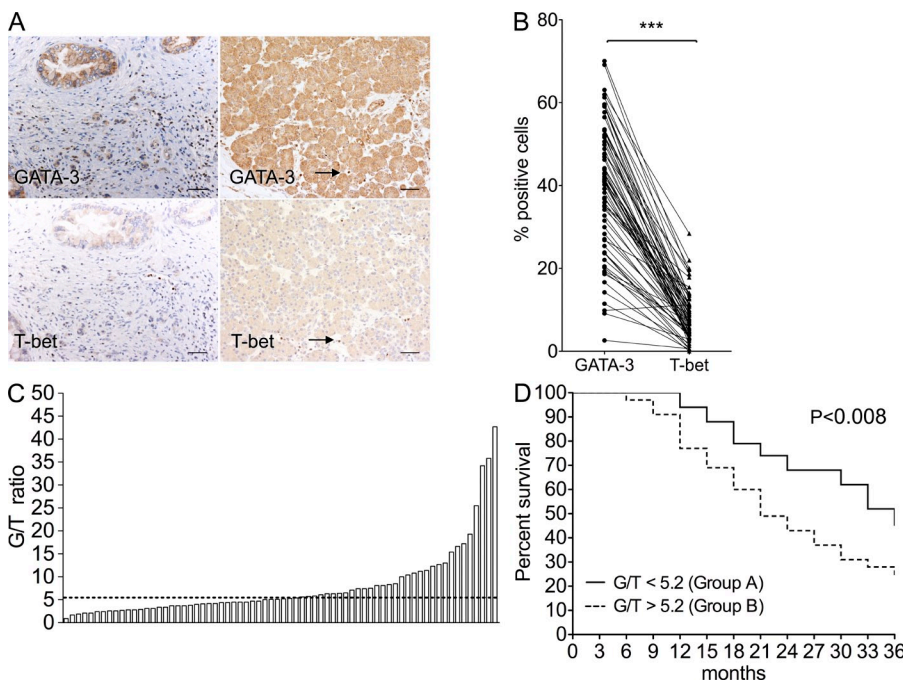To investigate the potential role of TSLP in driving Th2 immune deviation

Figure 1. The ratio of G/T tumor–infiltrating lymphoid cells predicts survival after surgery in patients with stage IB/III pancreatic cancer. (A) Representative immunohistochemical analysis for lymphoid GATA-3 and T-bet staining in the tumor (n = 69; left) and normal pancreatic tissue from benign lesions (n = 3; right). The arrows indicate rare positive cells in normal tissue. Bars, 100 µm. (B) Percentage of GATA-3+ (circles) and T-bet+ (triangles) lymphoid cells for each of the analyzed tumor samples (n = 69). The values are significantly different and indicated as: ***, P < 0.001 (determined by paired one-tailed Student's t test). (C) Waterfall plot of the G/T ratio for each tumor sample. The dashed line indicates the G/T ratio 5.2, which is the median value. (D) Kaplan-Meier curve for overall survival by median G/T ratio (5.2). Survival significantly decreased (P = 0.008) as a function of a G/T ratio ≥ 5.2.

Table I. Characteristics of the 69 patients grouped by the G/T ratio of tumor-infiltrating lymphoid cells

Variable	G/T ≤ 5.2 (*n* = 35)	G/T > 5.2 (*n* = 34)
Gender: female	18 (51%)	15 (44%)
Median age	64	57.5
Tumor site: head	31 (89%)	30 (88%)
Tumor size > 3 cm	9 (25%)	15 (44%)
Stage IIB/III	26 (74%)	31 (91%)
Grade 3	11 (31%)	12 (35%)
Karnofsky >80	24 (69%)	21 (62%)
Surgical margin R1	12 (34%)	15 (44%)
Median preoperative CA19.9	217 ± 3453.8 range (1–18,470)	94 ± 1342.6 range (1–6,832)
Median postoperative CA19.9	16 ± 88.8 range (1–416)	23 ± 678.6 range (0.1–3,745)
[a]Treatment: PEFG	18 (51%)	20 (59%)

[a]Patients who had R0 or R1 resection of a stage IB-III pancreatic cancer, aged 18–75 yr and Karnofsky Performance Status (KPS) > 60, were eligible for adjuvant therapy. The patients were required to have postoperative treatment initiation within 2 mo from surgery, no previous chemotherapy or radiotherapy for pancreatic cancer, and adequate bone marrow, liver, and kidney. After tumor resection, 31 patients were treated with gemcitabine (Burris et al., 1997) and 38 patients received the PEFG regimen consisting of cisplatin, epirubicin, gemcitabine, and 5-fluorouracil (Reni et al., 2005). In both cases, chemotherapy was administered for 3 mo followed by chemoradiation (Reni et al., 2005).

in pancreatic cancer, we evaluated, by real-time PCR, TSLP mRNA expression in tumor and macroscopically uninvolved surrounding tissues from surgical specimens, and in isolated and in vitro–cultured tumor cells and CAFs, as described in Materials and methods. CAF cell lines were obtained from surgical samples of 15 patients, and corresponding tumor cell lines from the same patients were obtained in five cases. Because normal human pancreatic fibroblasts were not available, human dermal fibroblasts (HDFs) from normal skin were used as control. All cell lines were tested after few passages in culture and their characterization is reported in Fig. S2. Although tumor cell lines, when established, could then be kept in long-term culture as stabilized lines, usually CAFs could not grow longer than nine passages. We found that TSLP was expressed in the tumor and, to a much lower extent, in the surrounding tissue (Fig. 2 A). Moreover, TSLP was expressed in CAFs but not in tumor cells and HDFs (Fig. 2 A). Expression of TSLP in the stroma, and not in tumor epithelial cells, was confirmed by laser capture microdissection (LCM; Fig. 2 B).

We then measured, by ELISA, TSLP secretion by CAFs after activation with proinflammatory cytokines known to induce TSLP production in epithelial cells (Lee and Ziegler, 2007), smooth muscle cells (Zhang et al., 2007), and skin keratinocytes (Bogiatzi et al., 2007). TSLP secretion, in the absence of activation, was observed in a limited number of CAFs and never in tumor cells and HDFs (unpublished data). TNF and IL-1β used as single agents or in combination strongly increased or induced a significantly higher TSLP secretion in CAFs than in HDFs. However, in agreement with the mRNA expression data, no TSLP production by tumor cells was observed (Fig. 2 C).

We then confirmed the presence of the proinflammatory cytokines in tumor samples (Fig. 2 D). TNF was expressed in the tumor at higher levels than in the corresponding surrounding tissue (Fig. 2 D, top), whereas IL-1β was expressed in both tissues with prevalence in one or the other depending on the sample (Fig. 2 D, bottom). The variability of expression

of TSLP (Fig. 2 A) and proinflammatory cytokines (Fig. 2 D) in the surrounding tissue is possibly related to its morphological characteristics that could vary among samples from conserved normal parenchyma to preexisting or associated obstructive pancreatitis.

To identify cells producing the proinflammatory cytokines, we tested their expression in tumor epithelial and stromal cells collected by LCM and in cultured paired tumor cells and CAFs from the same patient (Fig. 2 E). TNF was mainly expressed in tumor epithelial cells, compared with stroma cells, and not in CAFs (Fig. 2 E, left). IL-1β was expressed in both tumor compartments and, although at low levels, in CAFs (Fig. 2 E, right and inset). IL-1β secretion was confirmed by immunohistochemistry (unpublished data). As the two proinflammatory cytokines were expressed in tumor cells, we further tested whether treatment of CAFs with tumor cell supernatant induced TSLP secretion. CAFs, but not HDFs, treated with the tumor cell supernatant produced TSLP that was significantly inhibited by anti-TNF (34% inhibition) and anti–IL-1β (38% inhibition) Abs but not by an isotype control (Fig. 2 F). Collectively, these experiments demonstrate that TSLP expression is up-regulated in pancreatic cancer and released by CAFs under the influence of TNF and IL-1β that are expressed in pancreatic cancer and secreted by tumor cells.

Myeloid DCs are activated by the supernatant of proinflammatory cytokine–treated CAFs and acquire Th2–polarizing capability

We next evaluated, in vitro, the effects of the supernatant of activated CAFs on myeloid DC maturation and function (Fig. 3). DCs conditioned by CAF supernatant strongly up-regulated activation and maturation markers at levels comparable to or even higher than those of TSLP and Poly I:C (i.e., controls for DCs maturation; Fig. 3 A).

The potential role of CAF-released TSLP in DC activation/maturation was then investigated by looking at the expression of
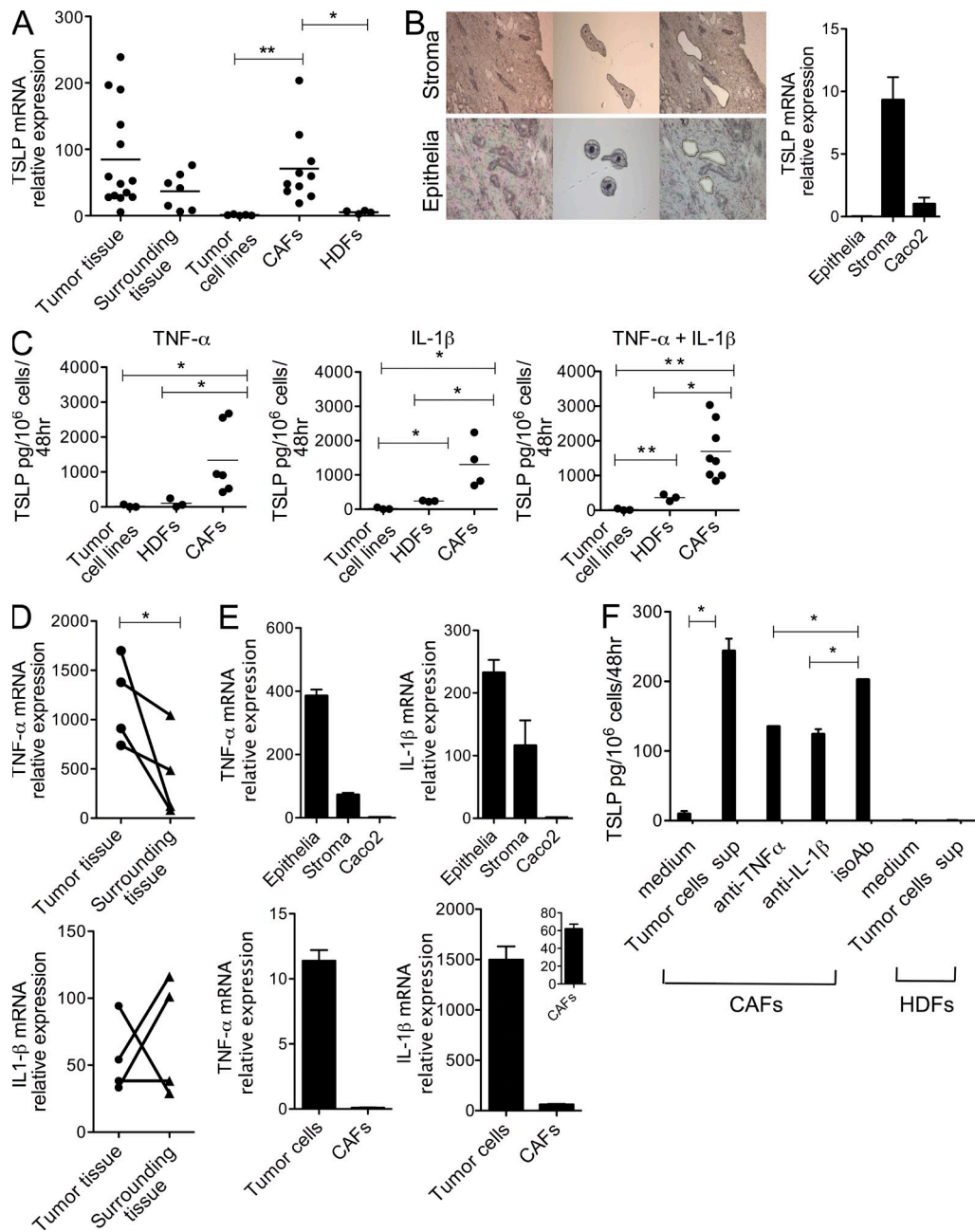
Figure 2. **TSLP is expressed by CAFs, and its secretion is induced by proinflammatory cytokines released by tumor cells.** (A) TSLP mRNA expression in tumor and surrounding tissues, tumor cell lines, CAFs, and HDFs. Each dot represents a different surgical sample or a different cell line. (B) TSLP is expressed in vivo in the stroma. LCM (left) was used to collect stromal (top) and epithelial (bottom) tumor cells from surgical specimens and TSLP mRNA expression analyzed (right; representative of tumor samples from three patients). The mRNA expression levels were normalized to the expression of GAPDH. TSLP mRNA expression of Caco2 cell line was used as calibrator, as in Rimoldi et al. (2005). (C) TSLP protein secretion by CAFs, HDFs, and tumor cell lines treated with proinflammatory cytokines as single agent or in combination. Left, 20 ng/ml TNF; middle, 10 ng/ml IL-1β; right, TNF plus IL-1β. Each dot represents a different cell line. (D) TNF (top) and IL-1β (bottom) mRNA expression in tumor and the corresponding surrounding tissue (each dot and corresponding triangle represent surgical samples from single patients). (E) TNF (left) and IL-1β (right) mRNA expression in tumor epithelial and stromal cells collected by LCM (top; representative of tumor samples from three patients) and in isolated and in vitro–cultured paired tumor cell lines and CAFs from the same patient (bottom; representative of tumor samples from three patients). Inset magnifies IL-1β expression in CAFs. (F) TSLP protein secretion by CAFs treated with supernatant from tumor cell lines (tumor cells sup) in the absence and presence of anti-TNF, anti-IL-1β, and isotype control Abs (representative of experiments performed with three different tumor cell lines and three CAFs). Data in A–F are means of at least duplicate determinations ± SD. Responses significantly different in A, C, D, and F are indicated as: *, P < 0.05; **, 0.001< P < 0.01 (determined by paired or unpaired one-tailed Student's t test).

the TSLP receptor (TSLPR), which is up-regulated in TSLP-treated DCs (Soumelis et al., 2002; Ito et al., 2005; Lu et al., 2009). We found that DCs treated with CAF supernatant expressed the TSPLR at higher levels than those treated with HDF supernatant (Fig. 3 B), indicating that a maturation stimulus for DC activation present in the CAF supernatant is TSLP. We further demonstrated that TSLP present in the supernatant was responsible for DC activation by experiments in which CD80 expression, whose up-regulation is particularly influenced by TSLP (Soumelis et al., 2002; Bogiatzi et al., 2007), was inhibited by the addition of an anti-TSLP Ab (Fig. 3 C).

We then measured the secretion of cytokines and chemokines by DCs either left untreated or treated with the supernatants of TNF-treated CAFs and HDFs. TNF and TSLP were used as controls. After 24 h, DCs were extensively washed to remove any exogenous or fibroblast-produced cytokine and left for a further 48 h in culture before collecting the supernatant. IL-12, IL-10, TNF, IL-1β, and IL-6 were not produced in any condition (unpublished data). The Th2 chemoattractants

thymus and activation-regulated chemokine (TARC/CCL17) and macrophage-derived chemokine (MDC/CCL22) were secreted as expected by TSLP-treated DCs and, importantly, by DCs conditioned with the supernatant of activated CAFs. In contrast, DCs conditioned with the supernatant of activated HDFs secreted MDC/CCL22 but not TARC/CCL17 (Fig. 3 D). Th1 chemoattractants RANTES/CCL5 and IP-10/CXCL10 were secreted exclusively by DCs conditioned with the HDF supernatant (Fig. 3 D).

To test their polarizing capability, DCs conditioned with the supernatant of TNF-treated CAFs were co-cultured with naive CD4$^+$CD45RA$^+$ T cells, purified from cord blood, in the absence or in the presence of neutralizing Abs. After 6 d, release of IFN-γ and IL-13 (as prototypic Th1 and Th2 cytokines, respectively) by activated CD4$^+$ T cells was assessed by ELISA (Fig. 3 E). TSLP-treated DCs, used as positive control, induced IL-13 as expected but not IFN-γ–producing CD4$^+$ T cells. Notably, DCs conditioned with CAF supernatant also induced secretion of IL-13 that was inhibited by an anti-TSLP (47% inhibition) but not an anti-TNF Ab. CD4$^+$ T cells activated with DCs cultured with medium alone or TNF or the supernatant of TNF-treated HDFs remained unpolarized (Fig. 3 E). Collectively, these data demonstrate that CAFs, via the release of TSLP, induce DCs with features of TSLP-treated DCs.
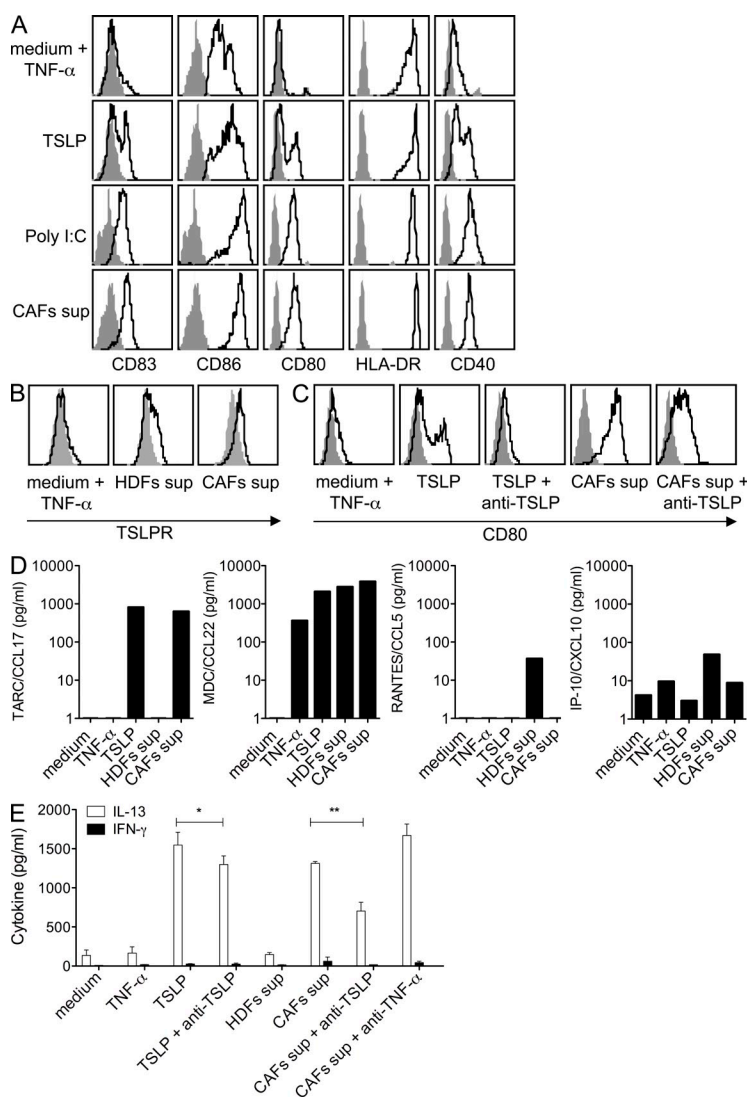

Figure 3. Supernatant of TNF-treated CAF (CAF sup) activates in vitro myeloid DCs with features of TSLP-treated DCs. (A) FACS analysis of DCs after 24-h incubation with the indicated stimuli (representative of independent experiments, $n = 3$). Experiments were performed with supernatants from three different CAFs. Open histograms represent staining of DC activation markers; filled histograms represent the isotype control. (B) FACS analysis of TSLPR expression by DCs activated in the presence of medium plus TNF, supernatant of TNF-treated HDF (HDF sup; obtained from two different HDFs), and CAF sup (obtained from three different CAFs; representative of independent experiments $n = 3$). (C) FACS analysis of CD80 expression by DCs incubated with CAF sup (obtained from three different CAFs) in the absence and in the presence of an anti-TSLP Ab (representative of independent experiments, $n = 4$). Experiments with medium plus TNF and TSLP, in the absence and in the presence of the anti-TSLP Ab, are shown as negative and positive controls, respectively. (D) Chemokine production by DCs activated with the following stimuli: medium alone, 20 ng/ml TNF; 15 ng/ml TSLP; HDF sup and CAF sup (representative of three experiments performed with three different CAFs and two different HDFs). (E) CAF sup endows DCs with Th2 polarizing capability that depends on TSLP. CD4$^+$CD45RA$^+$ naive T cells were cultured with DCs previously activated with the indicated stimuli. At day 6, IFN-γ and IL-13 secreted by CD4$^+$ T cells were tested by ELISA. When indicated, anti-TSLP and anti-TNF Abs were added in culture. Data are means of duplicate determinations ± SD and represent one of five experiments (performed with four different CAFs and two different HDFs). Release of IL-13 significantly lower in the presence of an anti-TSLP Ab are indicated as: *, P < 0.05; **, 0.001 < P < 0.01 (determined by unpaired one-tailed Student's t test).

DCs with features of TSLP–treated DCs and Th2–attracting chemokines are present in vivo in pancreatic cancer patients

Finally, we investigated, by immunohistochemistry and flow cytometry, the presence in vivo of TSLP-conditioned DCs, identified as CD11c⁺TSLPR⁺ cells. Myeloid DCs in the steady state express very low levels of TSLPR that is up-regulated in the presence of TSLP (Reche et al., 2001). Indeed, we found CD11c⁺TSLPR⁺ cells in the tumor (Fig. 4 A) and in draining but not in nondraining LNs (Fig. 4 B). These findings witness DC activation in vivo by a stimulus able to up-regulate the TSLPR. This evidence, along with the in vitro demonstration that CD80 expression by DCs conditioned by CAF supernatant depends on TSLP secretion (shown in Fig. 3 C), validates TSLP as the cytokine responsible for activation in the tumor of DCs with features of TSLP-treated DCs.

In our hypothesis, TSLP-conditioned DCs present in the draining LNs activate Th2 cells that then home to the tumor under the influence of Th2 attractant chemokines. Thus, we evaluated, by real-time PCR, mRNA expression of TARC/ CCL17 and MDC/CCL22 in tumor samples and found expression in the tumor but not in the corresponding surrounding tissue (Fig. 4 C). We then measured expression of the two cytokines in tumor epithelial and stromal cells collected by LCM and in cultured paired tumor cells and CAFs from the same patient (Fig. 4 D). We found expression of both cytokines in the stroma (Fig. 4 D, top). In addition, MDC/CCL22, as already described in ovarian cancer (Curiel et al., 2004), was also expressed in tumor epithelial cells (Fig. 4 D, right). As for TNF (Fig. 2 E), TARC/CCL17 and MDC/CCL22 expression in the stroma was not attributable to CAFs (Fig. 4 D, bottom) but, in agreement with our previous in vitro results (Fig. 3 D), was most likely attributable to inflammatory cells (e.g., DCs). Collectively, these results support our hypothesis that TSLP-conditioned DCs induced by CAF-secreted TSLP migrate to the draining LNs to prime Th2 cells that home to the tumor under the influence of Th2-attracting chemokines.

DISCUSSION

In this study, we first show that in pancreatic cancer the Th2 immune deviation has an active role in tumor progression, in that the quantity of Th2 with respect to Th1 cells present in the tumor stroma has a direct correlation with prognosis in surgically resected patients. Although tumor antigen–specific CD4⁺ Th2 cells have been already described in the blood of patients with different neoplastic diseases (Tatsumi et al., 2002, 2003; Slager et al., 2003; Marturano et al., 2008), to our knowledge this is the first demonstration of a statistically significant correlation between prevalent Th2 over Th1 tumor immune infiltrate and poor prognosis. Notably, statistical analysis proved that the ratio, rather than the absolute number, of GATA-3⁺ cells correlate with poor prognosis, pointing to the importance for the clinical outcome of the balance between Th2 and Th1 cells present in the tumor microenvironment.

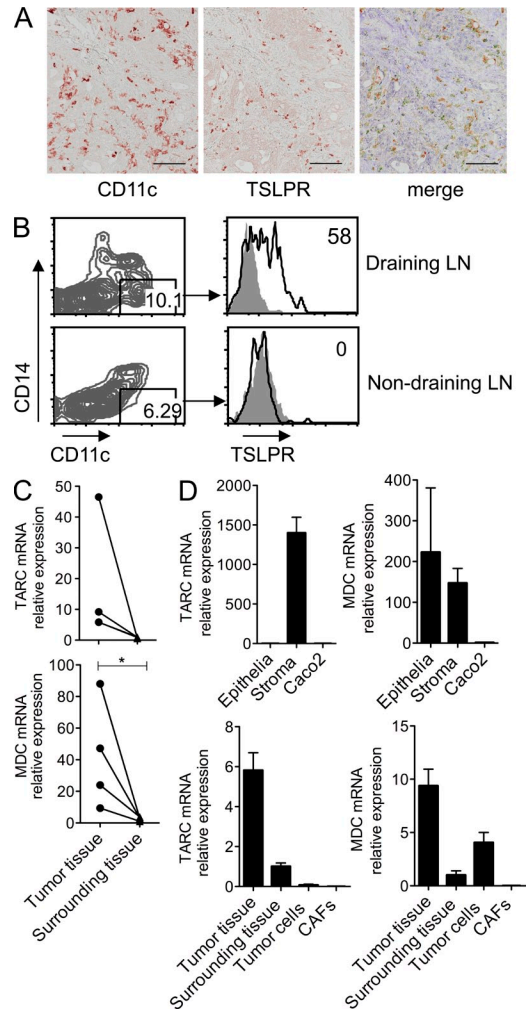Second, we addressed what leads to the Th2 immune deviation in pancreatic cancer and identified a central role for

Figure 4. TSLP-conditioned DCs and Th2-attractant chemokines are present in vivo. (A and B) TSLP-conditioned DCs are present in the tumor and in draining but not in nondraining LNs. (A) Immunohistochemical analysis for CD11c⁺TSLPR⁺ cells in the tumor representative of tumor samples from 10 patients. Bars, 100 µm. (B) FACS analysis of CD11c⁺TSLPR⁺CD14⁻ cells in draining (top) and corresponding nondraining (bottom) LNs representative of paired samples from four patients. Open histograms represent TSLPR staining; filled histograms represent the isotype control. Numbers indicate the percentage of gated (left) and positive (right) cells. (C and D) TARC/CCL17 and MDC/CCL22 mRNA expression in tumor and the corresponding surrounding tissue (C; each dot and corresponding triangle represent surgical samples from single patients), in tumor epithelial and stromal cells collected by LCM (D, top; representative of tumor samples from three patients), and in isolated and in vitro–cultured paired tumor cell lines and CAFs from the same patient (D, bottom; representative of tumor samples from three patients). Data in C and D are means of at least duplicate determinations ± SD. Responses significantly different are indicated as: *, P < 0.05 (determined by paired one-tailed Student's t test).

CAFs, which, through TSLP secretion, activate mDCs with features of TSLP-conditioned DCs with Th2-polarizing capability. Notably, DCs with the feature of TSLP-activated DCs (i.e., CD11c⁺TSLPR⁺) were found in vivo in the tumor stroma and in draining, but not in nondraining, LNs.

Previous studies addressed the presence of DCs in pancreatic cancer (Dallal et al., 2002; Fukunaga et al., 2004) with somewhat conflicting results. DCs were identified by anti-S100 staining in Fukunaga et al. (2004) and by anti-S100 and CD1a in Dallal et al. (2002). Dallal et al. (2002) found significant numbers of S100$^+$ or CD1a$^+$ cells in a very small percentage of patients. Compared with this paper, Fukunaga et al. (2004) identified patients with different levels of immune infiltration and found that infiltration of S100$^+$ cells paralleled infiltration by CD4$^+$ and CD8$^+$ T cells. The DC marker used in our study is different from the ones previously used. Because CD11c expression is not limited to DCs, it is possible that neutrophils and monocytes, which are possibly present in the tumor stroma, might also have been stained.

Cancer-related inflammation has been proposed as the seventh hallmark of cancer (Dunn et al., 2004; Grivennikov et al., 2010), and recently proinflammatory CAFs from a transgenic mouse tumor model were shown to orchestrate tumor-promoting inflammation in a NF-κB–dependent manner (Erez et al., 2010). In this scenario, our data identify a new molecule (i.e., TSLP) and a new function for CAFs in driving, under the influence of tumor cells, Th2-mediated inflammation that correlates with reduced survival in pancreatic cancer.

Collectively, based on our in vitro and in vivo data we propose a model of a complex cross talk among tumor cells, CAFs, Th2 cells, and possibly other immune cells favoring tumor promotion (Fig. S3). First, proinflammatory cytokines (TNF and IL-1β) are released by pancreatic tumor cells and elicit the release of TSLP by CAFs (Fig. S3 A). Secretion of these cytokines by pancreatic tumor cells has been previously reported (Arlt et al., 2002; Müerköster et al., 2004; Egberts et al., 2008). However, it is still unknown which signals are driving their secretion. Endogenous factors released by dead and dying tumor cells or present in the tumor microenvironment might serve as endogenous stimuli for NF-kB and inflammasome activation required for proinflammatory cytokine activation and release (Tschopp and Schroder, 2010; Fig. S3 A). Second, TSLP released by activated CAFs induces activation/maturation of tumor antigen–loaded resident DCs (Fig. S3, B and C). Third, activated DCs migrate to the draining LNs where they activate tumor antigen–specific CD4$^+$ Th2 cells (Fig. S3 D). Fourth, CD4$^+$ Th2 cells primed in the draining LNs home to the tumor under the influence of tumor-derived Th2 chemoattractants (TARC and MDC; Fig. S3 E). Fifth, recruited CD4$^+$GATA-3$^+$ Th2 cells may exert tumor-promoting effector functions (Fig. S3 F). Indeed, an altered balance between Th2 and Th1 cytokines present in the tumor microenvironment might further contribute to fibrosis. It has been shown that fibrogenesis is strongly linked with development of Th2 responses, and Th1 and Th2 cytokines exert opposing roles by promoting collagen degradation and synthesis, respectively (Wynn, 2004). Th2 cells might also promote differentiation of M2 macrophages both directly by tumor antigen–specific recognition of peptide–MHC class II complexes at the surface of differentiating monocytes and indirectly through Th2 cytokines release. The presence of M2-polarized

macrophages in pancreatic cancer has been reported (Kurahara et al., 2009), and we also have preliminary evidence of tumor stroma infiltration by CD68$^+$CD163$^+$ cells (unpublished data).

Clinical outcome in pancreatic cancer patients with resectable tumor is still disappointing with a median survival of 20–22 mo (Hidalgo, 2010). However, time to relapse and overall survival in this patient population may greatly vary, and few risk factors for recurrent disease have been defined so far (Hidalgo, 2010). In this paper, we identified the ratio of Th2/Th1 tumor-infiltrating lymphoid cells as an independent prognostic marker of survival that might be used for patient stratification in future prospective studies.

Notably, elucidation of the cytokine/chemokine network implicated in the Th2 immune deviation may allow for the design of innovative therapeutic strategies to complement currently available therapies (including therapeutic vaccination or adoptive immunotherapy) for pancreatic cancer based on proinflammatory cytokines and TSLP blocking strategies. Toward the feasibility of these approaches, clinical trials of TNF antagonists in advanced cancer patients have resulted in disease stabilization and some partial responses (Harrison et al., 2007; Mantovani et al., 2008). Clinical grade anti–IL-1β Abs are available to treat autoimmune and autoinflammatory diseases (van den Berg, 2000; Atzeni and Sarzi-Puttini, 2009; Lachmann et al., 2009) and, recently, treatment with an IL-1 inhibitor in patients with smoldering or indolent multiple myeloma at risk of progression to active myeloma was responsible for improved progression-free survival (Lust et al., 2009). Finally, concerning possible ways to silence TSLP, as a result of its role in allergy, several companies are already involved in developing clinical grade neutralizing Abs, which should be available for clinical applications in the near future (Edwards, 2008).

Future studies will address the mechanisms by which Th2 cells promote tumor progression and, specifically, which cellular and molecular interactions they use to do so within the tumor microenvironment. These studies will also possibly be conducted in animal models of spontaneous pancreatic cancer development recapitulating the different steps of pancreatic carcinogenesis from inception to invasive cancer paralleling the human disease (Hingorani et al., 2003; Leach, 2004). Furthermore, whether the mechanisms of Th2-mediated inflammation constitute a common phenomenon operative in multiple human tumors should also be investigated. Specifically, the role of TSLP and the ratio of G/T-infiltrating lymphocytes in other tumor types, either gastrointestinal or other epithelial tumors with important fibrotic component, should be addressed.

In summary, we identified in human pancreatic cancer a complex cross talk among tumor cells, CAFs, DCs, and T cells leading to Th2 inflammation, which significantly correlates with poor survival. Thus, therapeutic intervention aimed at interfering with this negative cross talk may prove to be beneficial for improving prognosis in pancreatic cancer patients.

MATERIALS AND METHODS

Patient population enrolled for survival analysis. 69 patients who had R0 or R1 resection of a stage IB-III pancreatic cancer, according to the 2002 staging criteria of the American Joint Commission on Cancer (Evans et al., 2002),

followed by different chemotherapeutic regimens and radiotherapy, were enrolled in the survival study. The characteristics of the patients are reported in Table I.

Tissue specimens and establishment of cell lines. Tumor and LN samples were collected at surgery. Surrounding tissue was sampled at least at a 1-cm distance from macroscopically evident neoplastic tissue. However, morphological characteristics varied among samples from conserved normal parenchyma to preexisting or associated obstructive pancreatitis. Normal pancreatic tissue was obtained from surgical samples of patients who underwent surgery for benign pancreatic lesions. The Institutional Ethics Committee (Comitato Etico Fondazione Centro San Raffaele del Monte Tabor, Istituto Scientifico Ospedale San Raffaele) had approved the study protocol, and written informed consent was obtained from all donors. Tumor specimens were in part frozen for RNA extraction and in part used for cell culture. Tumor pieces were cultured in IMDM medium (Lonza) plus 10% FBS, and after a few passages tumor cells and CAFs were separated with anti–fibroblast Ab–coated beads (Miltenyi Biotec). Draining and nondraining LNs were mashed in 2% FBS RPMI, 10 mM Hepes, and 400 U/ml collagenase D (Sigma-Aldrich).

Western blotting. Expression of α smooth muscle actin (SMA), pancytokeratin, and p53 by cultured CAFs and tumor cells was evaluated by Western blotting, as described in De Monte et al. (2008). Abs used were mouse anti–pan cytokeratin (Sigma-Aldrich), rabbit polyclonal anti–α-SMA (Abcam), mouse anti–p53 (DAKO), and mouse anti–β-actin (Sigma-Aldrich), followed by goat anti–mouse HRP or swine anti–rabbit HRP (DAKO), respectively. Immunodetection was performed by enhanced chemiluminescence (GE Healthcare), followed by autoradiography on Biomax films (Kodak).

Detection of K-ras mutations. Genomic DNA was extracted from 2×10^6 pancreatic cancer cells or CAFs with the QIAamp DNA mini kit (QIAGEN), and 30 ng of each sample was amplified for 40 cycles (58°C annealing temperature) with PFU-Turbo DNA polymerase (Agilent Technologies) with the following primers: Kras forward, 5′-GGTGGAGTATTTGATAGTG-TATTAAACC-3′; Kras reverse, 5′-TCATGAAAATGGTCAGAGA-AACC-3′. 283-bp PCR products containing k-ras codon 12 and 13 purified with QIAquick kit (QIAGEN) were then sequenced on both strands and analyzed with the FinchTv software (Geospiza).

LCM. Epithelial and stromal tumor cells were collected from frozen samples using the Arcturus LCM system, according to the manufacturer's instructions. The two tumor components, identified under microscopy, were cut and transferred on capsure HS caps and total RNA was extracted as described in the next section.

Real-time PCR. Total RNA was extracted using the PicoPure RNA isolation kit (Arcturus) or the RiboPure kit (Ambion), according to the manufacturers' instructions. 1 µg RNA was retro-transcribed with the High-Capacity cDNA reverse transcription kit (Applied Biosystems), and 10–50 ng cDNA was used for real-time PCR. To analyze the expression of different genes from RNA obtained by LCM a preamplification step was performed, according to the manufacturers' instructions. Assays on demand specific for human TSLP (Hs00263639-m1), IL-1β (Hs00174097-m1), TNF (Hs00174128), TARC/CCL17 (Hs00171074-m1), MDC/CCL22 (Hs99999075-m1), and GAPDH (Hs99999905-m1; Applied Biosystems) were used. Real-time PCR was performed on an AB7900HT machine (Applied Biosystems) using the S.D.S.2.1 program for the analysis. Fold induction among samples was calculated by $2^{-\Delta\Delta Ct}$ method. The target gene values were normalized with GAPDH values.

Fibroblasts stimulation and TSLP quantification. Fibroblasts were cultured overnight at 150.000–300.000 cells/ml in IMDM with 10% FBS, followed by 5–8 h of starving without serum. Medium was then replaced with IMDM with 2% FBS, and fibroblasts were cultured for 48 h with or without

the following stimuli: 20 ng/ml TNF, 10 ng/ml IL-1β, and supernatant from tumor cells. In inhibition experiments, 2 µg/ml anti-TNF, anti–IL-1β, or isotype-matched Abs (BD) were added. TSLP release was quantified by ELISA (R&D Systems).

Myeloid DC isolation and activation. Myeloid DCs were isolated from blood buffy coats of adult healthy donors after separation of mononuclear cells and enrichment in monocytes using density gradients as described in Recalde (1984). Monocytes were stained with anti-CD3, anti-CD19, anti-CD16, anti-CD14, anti-CD56 fluorescein (FITC), CD4-PE, and CD11c-APC–conjugated Abs. Lineage⁻CD4⁺CD11c⁺ cells were then isolated by sorting (MoFlo cell sorter; Beckman Coulter) with a purity of 97–99%. DCs were cultured at 10^6/ml in 96-well plates in 2% FBS IMDM with or without the following stimuli: 15 ng/ml TSLP (R&D Systems), 25 ng/ml poly I:C (Sigma-Aldrich), and supernatants of untreated or TNF-treated CAFs and HDFs. In inhibition experiments, 1 µg/ml anti-TSLP (R&D Systems) or 10 µg/ml anti-TNF (BD) Abs were added. After 24 h, DCs were washed and left for a further 48 h in culture. Cytokine and chemokines release in DC supernatants was measured by human chemokines and the inflammatory cytokines CBA (BD) or ELISA (TARC/CCL17 and MDC/CCL22; R&D Systems).

FACS analysis. DCs were stained with anti-CD80, anti-CD83, anti-HLA-DR, anti-CD86, and anti-CD40 Abs conjugated with either FITC or PE (BD) and anti-TSLPR, followed by biotinylated anti–mouse IgG, and then with streptavidin-PE or −PE-Cy5 (BioLegend). Samples were acquired with FACSCalibur (BD).

DC/T cell co-culture. Naive CD4⁺ T cells were purified from cord blood with anti-CD4–coated beads (Miltenyi Biotec), obtaining ≥90% CD4⁺CD45RA⁺ cells. Activated DCs were added to naive CD4⁺ T cells (5×10^4/well) at a 1:5 ratio in 96-well plates. After 6 d, supernatants were tested for IL-13 and IFN-γ release by ELISA (Mabtech).

Immunohistochemical analysis. Immunohistochemistry was performed on tissue sections from surgical specimens, as detailed in Tassi et al. (2008). The following Abs were used: anti–T-bet and anti–IL-1β (Santa Cruz Biotechnology, Inc.), anti–GATA-3 (R&D Systems), anti-CD11c (Novocastra), and anti-TSLPR (BioLegend). For GATA-3 and T-bet evaluation, immunostained slides were digitalized with the Aperio slide scanner and corresponding tumor areas on adjacent sections were selected. Lymphocytes with nuclear staining were counted using the IHC Nuclear Image Analysis algorithm of the Spectrum Plus software (Aperio) and normalized to a 1-mm² area. CD11c and TSLPR coexpression was visualized using a sequential immunoperoxidase labeling and erasing technique (Glass et al., 2009) with the alcohol-soluble peroxidase substrate 3-amino-9-ethylcarbazole, combined with an antibody-antigen elution after the first antibody reaction.

Statistical analysis. The survival curves were estimated with univariate analyses according to the Kaplan-Meier method and compared using the log-rank test. Univariate and multivariate analyses by the Cox proportional hazard model were performed to estimate the independent potential risk factors that influence disease-free survival and overall survival. All the probability values were from two-sided tests. Analyses were performed using the Statistica 4.0 statistical package for Windows (Statsoft).

Online supplemental material. Fig. S1 shows a scatter plot analysis of overall survival and G/T ratio. Fig. S2 shows the characteristics of cell lines used in the study. Fig. S3 depicts a model of cross talk among tumor cells, CAFs, and DCs driving Th2 inflammation in pancreatic cancer. Online supplemental material is available at http://www.jem.org/cgi/content/full/jem.20101876/DC1.

REFERENCES

Arlt, A., J. Vorndamm, S. Müerköster, H. Yu, W.E. Schmidt, U.R. Fölsch, and H. Schäfer. 2002. Autocrine production of interleukin 1beta confers constitutive nuclear factor kappaB activity and chemoresistance in pancreatic carcinoma cell lines. *Cancer Res.* 62:910–916.

Atzeni, F., and P. Sarzi-Puttini. 2009. Anti-cytokine antibodies for rheumatic diseases. *Curr. Opin. Investig. Drugs.* 10:1204–1211.

Bogiatzi, S.I., I. Fernandez, J.C. Bichet, M.A. Marloie-Provost, E. Volpe, X. Sastre, and V. Soumelis. 2007. Cutting edge: proinflammatory and Th2 cytokines synergize to induce thymic stromal lymphopoietin production by human skin keratinocytes. *J. Immunol.* 178:3373–3377.

Burris, H.A. III, M.J. Moore, J. Andersen, M.R. Green, M.L. Rothenberg, M.R. Modiano, M.C. Cripps, R.K. Portenoy, A.M. Storniolo, P. Tarassoff, et al. 1997. Improvements in survival and clinical benefit with gemcitabine as first-line therapy for patients with advanced pancreas cancer: a randomized trial. *J. Clin. Oncol.* 15:2403–2413.

Curiel, T.J., G. Coukos, L. Zou, X. Alvarez, P. Cheng, P. Mottram, M. Evdemon-Hogan, J.R. Conejo-Garcia, L. Zhang, M. Burow, et al. 2004. Specific recruitment of regulatory T cells in ovarian carcinoma fosters immune privilege and predicts reduced survival. *Nat. Med.* 10:942–949. doi:10.1038/nm1093

Dallal, R.M., P. Christakos, K. Lee, S. Egawa, Y.I. Son, and M.T. Lotze. 2002. Paucity of dendritic cells in pancreatic cancer. *Surgery.* 131:135–138. doi:10.1067/msy.2002.119937

De Monte, L., F. Sanvito, S. Olivieri, F. Viganò, C. Doglioni, M. Frasson, M. Braga, A. Bachi, P. Dellabona, M.P. Protti, and M. Alessio. 2008. Serological immunoreactivity against colon cancer proteome varies upon disease progression. *J. Proteome Res.* 7:504–514. doi:10.1021/pr070360m

Dunn, G.P., L.J. Old, and R.D. Schreiber. 2004. The three Es of cancer immunoediting. *Annu. Rev. Immunol.* 22:329–360. doi:10.1146/annurev.immunol.22.012703.104803

Edwards, M.J. 2008. Therapy directed against thymic stromal lymphopoietin. *Drug News Perspect.* 21:312–316. doi:10.1358/dnp.2008.21.6.1246830

Egberts, J.H., V. Cloosters, A. Noack, B. Schniewind, L. Thon, S. Klose, B. Kettler, C. von Forstner, C. Kneitz, J. Tepel, et al. 2008. Anti-tumor necrosis factor therapy inhibits pancreatic tumor growth and metastasis. *Cancer Res.* 68:1443–1450. doi:10.1158/0008-5472.CAN-07-5704

Erez, N., M. Truitt, P. Olson, S.T. Arron, and D. Hanahan. 2010. Cancer-associated fibroblasts are activated in incipient neoplasia to orchestrate tumor-promoting inflammation in an NF-kappaB–dependent manner. *Cancer Cell.* 17:135–147. doi:10.1016/j.ccr.2009.12.041

Evans, D.B., C. Charnsangavei, C. Fernandez-del-Castillo, Y. Fong, G.Y. Lauwers, et al. 2002. Exocrine pancreas. *In* AJCC Cancer Staging Manual. F.L. Greene, D.L. Page, I.D. Fleming, A.G. Fritz, C.M. Balch, D.G. Haller, and M. Morrow, editors. Springer, New York. 157-164.

Fukunaga, A., M. Miyamoto, Y. Cho, S. Murakami, Y. Kawarada, T. Oshikiri, K. Kato, T. Kurokawa, M. Suzuoki, Y. Nakakubo, et al. 2004. CD8+ tumor-infiltrating lymphocytes together with CD4+ tumor-infiltrating lymphocytes and dendritic cells improve the prognosis of patients with pancreatic adenocarcinoma. *Pancreas.* 28:e26–e31. doi:10.1097/00006676-200401000-00023

Glass, G., J.A. Papin, and J.W. Mandell. 2009. SIMPLE: a sequential immunoperoxidase labeling and erasing method. *J. Histochem. Cytochem.* 57:899–905. doi:10.1369/jhc.2009.953612

Grivennikov, S.I., F.R. Greten, and M. Karin. 2010. Immunity, inflammation, and cancer. *Cell.* 140:883–899. doi:10.1016/j.cell.2010.01.025

Harrison, M.L., E. Obermueller, N.R. Maisey, S. Hoare, K. Edmonds, N.F. Li, D. Chao, K. Hall, C. Lee, E. Timotheadou, et al. 2007. Tumor necrosis factor alpha as a new target for renal cell carcinoma: two sequential phase II trials of infliximab at standard and high dose. *J. Clin. Oncol.* 25:4542–4549. doi:10.1200/JCO.2007.11.2136

Hidalgo, M. 2010. Pancreatic cancer. *N. Engl. J. Med.* 362:1605–1617. doi:10.1056/NEJMra0901557

Hingorani, S.R., E.F. Petricoin, A. Maitra, V. Rajapakse, C. King, M.A. Jacobetz, S. Ross, T.P. Conrads, T.D. Veenstra, B.A. Hitt, et al. 2003. Preinvasive and invasive ductal pancreatic cancer and its early detection in the mouse. *Cancer Cell.* 4:437–450. doi:10.1016/S1535-6108(03)00309-X

Ito, T., Y.H. Wang, O. Duramad, T. Hori, G.J. Delespesse, N. Watanabe, F.X. Qin, Z. Yao, W. Cao, and Y.J. Liu. 2005. TSLP-activated dendritic cells induce an inflammatory T helper type 2 cell response through OX40 ligand. *J. Exp. Med.* 202:1213–1223. doi:10.1084/jem.20051135

Joyce, J.A., and J.W. Pollard. 2009. Microenvironmental regulation of metastasis. *Nat. Rev. Cancer.* 9:239–252. doi:10.1038/nrc2618

Kleeff, J., P. Beckhove, I. Esposito, S. Herzig, P.E. Huber, J.M. Löhr, and H. Friess. 2007. Pancreatic cancer microenvironment. *Int. J. Cancer.* 121:699–705. doi:10.1002/ijc.22871

Kurahara, H., H. Shinchi, Y. Mataki, K. Maemura, H. Noma, F. Kubo, M. Sakoda, S. Ueno, S. Natsugoe, and S. Takao. 2009. Significance of M2-polarized tumor-associated macrophage in pancreatic cancer. *J. Surg. Res.* 10.1016/j.jss.2009.05.026.

Lachmann, H.J., I. Kone-Paut, J.B. Kuemmerle-Deschner, K.S. Leslie, E. Hachulla, P. Quartier, X. Gitton, A. Widmer, N. Patel, and P.N. Hawkins; Canakinumab in CAPS Study Group. 2009. Use of canakinumab in the cryopyrin-associated periodic syndrome. *N. Engl. J. Med.* 360:2416–2425. doi:10.1056/NEJMoa0810787

Leach, S.D. 2004. Mouse models of pancreatic cancer: the fur is finally flying! *Cancer Cell.* 5:7–11. doi:10.1016/S1535-6108(03)00337-4

Lee, H.C., and S.F. Ziegler. 2007. Inducible expression of the proallergic cytokine thymic stromal lymphopoietin in airway epithelial cells is controlled by NFkappaB. *Proc. Natl. Acad. Sci. USA.* 104:914–919. doi:10.1073/pnas.0607305104

Liu, Y.J., V. Soumelis, N. Watanabe, T. Ito, Y.H. Wang, Rde.W. Malefyt, M. Omori, B. Zhou, and S.F. Ziegler. 2007. TSLP: an epithelial cell cytokine that regulates T cell differentiation by conditioning dendritic cell maturation. *Annu. Rev. Immunol.* 25:193–219. doi:10.1146/annurev.immunol.25.022106.141718

Lu, N., Y.H. Wang, Y.H. Wang, K. Arima, S. Hanabuchi, and Y.J. Liu. 2009. TSLP and IL-7 use two different mechanisms to regulate human CD4$^+$ T cell homeostasis. *J. Exp. Med.* 206:2111–2119. doi:10.1084/jem.20090153

Lust, J.A., M.Q. Lacy, S.R. Zeldenrust, A. Dispenzieri, M.A. Gertz, T.E. Witzig, S. Kumar, S.R. Hayman, S.J. Russell, F.K. Buadi, et al. 2009. Induction of a chronic disease state in patients with smoldering or indolent multiple myeloma by targeting interleukin 1beta-induced interleukin 6 production and the myeloma proliferative component. *Mayo Clin. Proc.* 84:114–122. doi:10.4065/84.2.114

Mahadevan, D., and D.D. Von Hoff. 2007. Tumor-stroma interactions in pancreatic ductal adenocarcinoma. *Mol. Cancer Ther.* 6:1186–1197. doi:10.1158/1535-7163.MCT-06-0686

Mantovani, A., P. Allavena, A. Sica, and F. Balkwill. 2008. Cancer-related inflammation. *Nature.* 454:436–444. doi:10.1038/nature07205

Marturano, J., R. Longhi, V. Russo, and M.P. Protti. 2008. Endosomal proteases influence the repertoire of MAGE-A3 epitopes recognized in vivo by CD4+ T cells. *Cancer Res.* 68:1555–1562. doi:10.1158/0008-5472.CAN-07-5233

Müerköster, S., K. Wegehenkel, A. Arlt, M. Witt, B. Sipos, M.L. Kruse, T. Sebens, G. Klöppel, H. Kalthoff, U.R. Fölsch, and H. Schäfer. 2004. Tumor stroma interactions induce chemoresistance in pancreatic ductal carcinoma cells involving increased secretion and paracrine effects of nitric oxide and interleukin-1beta. *Cancer Res.* 64:1331–1337. doi:10.1158/0008-5472.CAN-03-1860

Recalde, H.R. 1984. A simple method of obtaining monocytes in suspension. *J. Immunol. Methods.* 69:71–77. doi:10.1016/0022-1759(84)90278-3

Reche, P.A., V. Soumelis, D.M. Gorman, T. Clifford, Liu Mr, M. Travis, S.M. Zurawski, J. Johnston, Y.J. Liu, H. Spits, et al. 2001. Human thymic stromal lymphopoietin preferentially stimulates myeloid cells. *J. Immunol.* 167:336–343.

Reni, M., P. Passoni, E. Bonetto, G. Balzano, M.G. Panucci, A. Zerbi, M. Ronzoni, C. Staudacher, E. Villa, and V. Di Carlo. 2005.

Final results of a prospective trial of a PEFG (Cisplatin, Epirubicin, 5-Fluorouracil, Gemcitabine) regimen followed by radiotherapy after curative surgery for pancreatic adenocarcinoma. *Oncology.* 68:239–245. doi:10.1159/000086780

Rimoldi, M., M. Chieppa, V. Salucci, F. Avogadri, A. Sonzogni, G.M. Sampietro, A. Nespoli, G. Viale, P. Allavena, and M. Rescigno. 2005. Intestinal immune homeostasis is regulated by the crosstalk between epithelial cells and dendritic cells. *Nat. Immunol.* 6:507–514. doi:10.1038/ni1192

Slager, E.H., M. Borghi, C.E. van der Minne, C.A. Aarnoudse, M.J. Havenga, P.I. Schrier, S. Osanto, and M. Griffioen. 2003. CD4+ Th2 cell recognition of HLA-DR-restricted epitopes derived from CAMEL: a tumor antigen translated in an alternative open reading frame. *J. Immunol.* 170:1490–1497.

Soumelis, V., P.A. Reche, H. Kanzler, W. Yuan, G. Edward, B. Homey, M. Gilliet, S. Ho, S. Antonenko, A. Lauerma, et al. 2002. Human epithelial cells trigger dendritic cell–mediated allergic inflammation by producing TSLP. *Nat. Immunol.* 3:673–680. doi:10.1038/ni805

Tassi, E., F. Gavazzi, L. Albarello, V. Senyukov, R. Longhi, P. Dellabona, C. Doglioni, M. Braga, V. Di Carlo, and M.P. Protti. 2008. Carcinoembryonic antigen-specific but not antiviral CD4+ T cell immunity is impaired in pancreatic carcinoma patients. *J. Immunol.* 181:6595–6603.

Tatsumi, T., L.S. Kierstead, E. Ranieri, L. Gesualdo, F.P. Schena, J.H. Finke, R.M. Bukowski, J. Mueller-Berghaus, J.M. Kirkwood, W.W. Kwok, and W.J. Storkus. 2002. Disease-associated bias in T helper type 1 (Th1)/Th2 CD4^{+} T cell responses against MAGE-6 in HLA-DRB10401^{+} patients with renal cell carcinoma or melanoma. *J. Exp. Med.* 196:619–628. doi:10.1084/jem.20012142

Tatsumi, T., C.J. Herrem, W.C. Olson, J.H. Finke, R.M. Bukowski, M.S. Kinch, E. Ranieri, and W.J. Storkus. 2003. Disease stage variation in CD4+ and CD8+ T-cell reactivity to the receptor tyrosine kinase EphA2 in patients with renal cell carcinoma. *Cancer Res.* 63:4481–4489.

Tschopp, J., and K. Schroder. 2010. NLRP3 inflammasome activation: The convergence of multiple signalling pathways on ROS production? *Nat. Rev. Immunol.* 10:210–215. doi:10.1038/nri2725

van den Berg, W.B. 2000. Arguments for interleukin 1 as a target in chronic arthritis. *Ann. Rheum. Dis.* 59:i81–i84. doi:10.1136/ard.59.suppl_1.i81

Wynn, T.A. 2004. Fibrotic disease and the T(H)1/T(H)2 paradigm. *Nat. Rev. Immunol.* 4:583–594. doi:10.1038/nri1412

Zhang, K., L. Shan, M.S. Rahman, H. Unruh, A.J. Halayko, and A.S. Gounni. 2007. Constitutive and inducible thymic stromal lymphopoietin expression in human airway smooth muscle cells: role in chronic obstructive pulmonary disease. *Am. J. Physiol. Lung Cell. Mol. Physiol.* 293:L375–L382. doi:10.1152/ajplung.00045.2007